

Supplementary Materials for

Mast cell activation in lungs during SARS-CoV-2 infection associated with lung pathology and severe COVID-19

Janessa Y. J. Tan^{*1}, Danielle E. Anderson^{*1,2,3}, Abhay P. S. Rathore⁴, Aled O'Neill¹, Chinmay Kumar Mantri¹, Wilfried A. A. Saron¹, Cheryl Q.E. Lee⁵, Chu Wern Cui⁵, Adrian E. Z. Kang¹, Randy Foo¹, Shirin Kalimuddin^{1,6}, Jenny G. Low^{1,6}, Lena Ho⁵, Paul Tambyah^{7,8}, Thomas W. Burke⁹, Christopher W. Woods^{9,10}, Kuan Rong Chan¹, Jörn Karhausen^{4,11}, Ashley L. St. John^{1,4,12,13**}

¹Program in Emerging Infectious Diseases, Duke-NUS Medical School, Singapore

²The Peter Doherty Institute for Infection and Immunity, University of Melbourne, Melbourne, Victoria, 3000, Australia[#]

³Victorian Infectious Diseases Reference Laboratory, Melbourne, Victoria, 3000, Australia[#]

⁴Department of Pathology, Duke University Medical Center, Durham, NC, USA

⁵Duke-NUS Medical School, Program in Cardiovascular and Metabolic Disorders, Singapore

⁶Department of Infectious Diseases, Singapore General Hospital, Singapore

⁷Infectious Diseases Translational Research Programme, Department of Medicine, Yong Loo Lin School of Medicine, National University of Singapore, 119228 Singapore, Singapore

⁸Division of Infectious Disease, University Medicine Cluster, National University Hospital, Singapore

⁹Center for Applied Genomics and Precision Medicine, Duke University Medical Center, Durham, NC, USA

¹⁰Division of Infectious Diseases, Duke University Medical Center; Durham VA Medical Center, Durham, NC, USA

¹¹Department of Anesthesiology, Duke University Medical Center, Durham, NC, USA

¹²Department of Microbiology and Immunology, National University of Singapore, Singapore

¹³SingHealth Duke-NUS Global Health Institute, Singapore

Correspondence to: ashley.st.john@duke-nus.edu.sg

This PDF file includes:

Materials and Methods

Figs. S1 to S7

Table S1 to S3

Materials and Methods

SARS-CoV-2 Propagation

Vero-E6 cells (ATCC®CRL-1586TM, 7.5×10^5 cells/mL) were infected with SARS-CoV-2 isolate hCoV-19/Singapore/2/2020 (WX-56) (GISAID accession ID: EPI_ISL_407987) at a multiplicity of infection (MOI) of 0.01 MOI for 1h at 37°C, 5% CO₂. After infection, 8 mL of DMEM medium with 5% fetal bovine serum (FBS) was added. Supernatant was harvested 3 days post infection. The ancestral SARS-CoV-2 strain used to identify whether MCs contribute directly to the pathological changes observed in lung tissue, SARS-CoV-2/Australia/Vic/01/20 was propagated in Vero-TMPRSS2 cells cultured with DMEM supplemented with 5% FBS and 1% penicillin/streptomycin at 37°C. Cell culture supernatants were harvested, centrifuged and aliquoted once cytopathic effect (CPE) was observed. Viral titres were determined by limited dilution using the Spearman-Kärber method(1). For plaque assays, Vero-E6 were seeded into 6-well plates (6×10^5 cells/well) and incubated overnight at 37°C, 5% CO₂ to achieve 90-100% confluence. SARS-CoV-2 isolate WX-56 was diluted up to 10^{-6} with 2% FBS DMEM medium. Cells were washed with 1mL PBS before infecting with 100 μ L of diluted virus. The plate was incubated at 37°C, 5% CO₂ for 1h and rotated every 15 min to prevent the cells from drying. After incubation, 3 mL of carboxymethylcellulose (CMC) was added to each well and incubated further for 3 days at 37°C, 5% CO₂. The plate was fixed using 4% paraformaldehyde and stained with crystal violet 3 days post infection. To quantify virus using a median tissue culture infectious dose-50 (TCID₅₀) assay, Vero-E6 (2×10^4 cells/mL) were seeded into 96-well plates (1×10^4 cells/well) in quadruplets and incubated overnight at 37°C, 5% CO₂ to achieve 90-100% confluence. SARS-CoV-2 isolate WX-56 was diluted up to 10^{-8} with 5% FBS DMEM medium. Serially diluted virus (100 μ L) was added to each well and incubated for 4 days before wells showing CPE were counted to determine the virus titer.

Adeno-associated virus (AAV) production, purification and administration

Viruses were produced as per standard protocol(2). Briefly, AAVs were packaged via triple transfection of HEK293 cells. HEK293 cells were seeded in 10%FBS/DMEM supplemented with glutaMax (ThermoFisher Scientific #35050061), pyruvate, (ThermoFisher Scientific # 11360070) and MEM non-essential amino acids (Gibco # 11140050). Confluency at transfection was between 70–90%. Media was replaced with fresh pre-warmed growth media before transfection. For each HYPERFlask 'M' (Corning #CLS10034), 300 μ g of pHHelper (Cell Biolabs), 150 μ g of pRepCap (encoding AAV9 (UPenn Vector Core)), and 150 μ g of pAAV (containing the ITR-cargo-ITR) were mixed in 7 ml of DMEM, followed by mixing with 2.8 mg of PEI "MAX" 40k (Polysciences # 24765-1). The mixture was incubated at room temperature for 15 min, and transferred drop wise to the cell media. The day after transfection, the media was changed to DMEM containing 2%FBS, glutaMax, pyruvate, and MEM non-essential amino acids. Cells were harvested 48-72 hrs after transfection by dissociation with 5 mM EDTA in PBS (pH7.2), and pelleted at $1500 \times g$ for 12 min. Cell pellets were resuspended in 5 ml of lysis buffer (Tris HCl pH 7.5, 2 mM MgCl₂, 150 mM NaCl), and freeze-thawed three times between a dry ice-ethanol bath and a 37°C water bath. Cell debris was clarified by centrifuging $4000 \times g$ for 5 min, and the supernatant collected. The collected supernatant was treated with 50 U/ml of Benzonase (Sigma-Aldrich) and 1 U/ml of RNase cocktail (Invitrogen # 10638255) for 30 min at 37°C to remove unpackaged nucleic acids. After incubation, the lysate was loaded on a discontinuous density gradient consisting of 4 mL, 6 mL, 7 mL, and 4 mL of 15%, 25%, 40%, and 60% Optiprep (Sigma-Aldrich # D1556) respectively in a 29.9 mL Optiseal polypropylene tube (Beckman-Coulter # 361625). The tubes were ultracentrifuged at 54,000 rpm, at 18 °C, for 1.5 h, on a Type 70 Ti rotor. The 40% fraction was extracted, and dialyzed with 0.001% pluronic acid/PBS, using Amicon Ultra-15 (100 kDa MWCO)(Millipore # UFC910024). The titre of the purified AAV9-hACE2 vector stocks were determined using real-time qPCR with ITR-sequence-specific primers and probe(3), referenced against the ATCC reference standard material 8 (ATCC).

C57Bl/6 and *Kit^{W-sh/W-sh}* mice that were treated with AAV9-hACE2 were purchased from InVivos, Singapore, and housed in the Duke-NUS Vivarium prior to use. Mice were anesthetized with xylazine/ketamine and inoculated intranasally with 1×10^{11} PFU of AA9-ACE2 delivered in 30 μ L, alternating droplets between both nares. SARS-CoV-2 infections were performed 21 days later to allow maximal expression of hACE2.

SARS-CoV-2 Infection of NHPs

Cynomolgus macaques (*Macaca fascicularis*) were used for NHP studies. Cynomolgus macaques were purchased from the SingHealth colony and free of antibodies against CoV. Infection studies were performed under BSL3 containment in the Duke-NUS Medical School ABSL3 facility. Prior to infection, NHPs were implanted with temperature transponders (Star-Oddi, Iceland). Body temperature was monitored every 15 min using a surgically implanted temperature sensor and rectally whenever the animals were anesthetized. For infection and sampling, animals were sedated with an intramuscular injection of ketamine (10-15 mg/kg) and medetomidine (0.05 mg/kg). Weight was recorded and a physical inspection was performed. Following initial sedation, 5% isoflurane was applied to achieve deeper anesthesia. A laryngoscope was used to intubate using an endotracheal (ET) tube. A 3 ml disposable luer lock syringe with 100 μ l 3×10^7 TCID₅₀/mL of SARS-CoV-2 isolate WX-56 was attached to ET tube connector for intratracheal infection. After injecting the virus, the ET tube was flushed with 1 ml of PBS to clear any residual inoculum. Animals were extubated and IV atipamezole was given to partially reverse medetomidine and facilitate faster recovery of the animals.

Post-infection, animals were observed twice daily for activity and observation of clinical signs. At days 0, 1, 3, 5, 7, 9, 14 and 21 post-infection, the animals were anesthetized and intubated using the same technique used for infection. Animals were weighed and blood samples were collected from the femoral vein in CPT tubes. Nasal, rectal, throat and eye swabs were collected. Nasal rinse and lung lavage were performed with 500 μ l and 6 ml PBS, respectively. The NHPs were euthanized at 21 days post-infection to allow for a full necropsy. Gross tissue observations were characterized by veterinarians and recorded upon necropsy. Blood, CSF, and tissues were harvested for RNA detection and histology.

RNA isolation from mouse and primate tissues and PCR-based quantification of SARS-CoV-2

Organs harvested from AAV-hACE2 knocked-in mice and NHPs were transferred to Lysing Matrix Y tubes (MPBio, #116960050-CF) containing 0.5 mm diameter Ytria-Stabilized Zirconium Oxide beads. 500 μ L 5% FBS DMEM was added into each tube and tissues were homogenized with a handheld homogenizer (MPBio SuperFastPrep-1) for 1 min. Total RNA was extracted from all samples using E.Z.N.A. Total RNA Kit I (Omega Bio-tek) or QIAamp Viral RNA Mini Kit (Qiagen, Germany) according to the manufacturer's instructions and samples were analyzed by real-time quantitative reverse transcription-PCR (RT-qPCR) for the detection of SARS-CoV-2 in mouse and NHP samples as previously described(4, 5).

Assay	Oligonucleotide	Sequence
N gene	N_Sarbeco_F	CACATTGGCACCCGCAATC
	N_Sarbeco_P	FAM- ACTTCCTCAAGGAACAACATTGCCA- BBQ
	N_Sarbeco_R	GAGGAACGAGAAGAGGCTTG

Five SARS-CoV-2 quantitation standards (1.9×10^7 , 1.7×10^6 , 1.8×10^5 , 1.6×10^4 , 1.5×10^3 RNA copies/mL) were included to determine genome copy number per mL of RNA.

Serum neutralizing antibody measurement in NHP by competitive ELISA.

The cPass™ SARS-CoV-2 Surrogate Virus Neutralization Test Kit (GenScript) was used according to manufacturer's instructions. Briefly, each serum sample was diluted 1:10 in Sample Dilution Buffer and incubated with an equal volume of HRP-RBD solution for 30 min at 37°C. The mix was then applied to strips pre-coated with ACE2 protein for 15 min at 37°C. RBD-ACE2 binding was visualized by addition of TMB substrate for 15 min at room temperature. The reaction was terminated using Stop Solution and absorbance measured at 450 nm. Inhibition of RBD-ACE2 binding was calculated using the formula: $(1 - (\text{OD value of sample})/(\text{OD value of negative control})) \times 100\%$.

Infection of AAV-hACE2 knock-in mice with SARS-CoV-2

AAV-hACE2 knock-in mice were transferred to either the Duke-NUS ABSL3 facility or Physical Containment Level 3 (PC3) facility AgriBio, Centre for AgriBioscience, Bundoora, Australia for SARS-CoV-2 infections. Mice were anesthetized with isoflurane for nasal inoculations. They were infected with

6×10^5 TCID₅₀/mL of SARS-CoV-2 isolate WX-56 via nasal inoculation (6 μ L per nostril) and were subsequently weighed daily. Mice transferred to PC3 facility were lightly anesthetized with isoflurane and transduced intranasally with AAV-hACE2 in a volume of 75 μ L. At 4-days post-transduction, mice were lightly anesthetized with isoflurane and inoculated intranasally with 1×10^5 TCID₅₀ of SARS-CoV-2/Australia/Vic/01/20 in a volume of 50 μ L. Blood was collected on 1, 3, 5 and 7-days post-infection via cheek bleed. Mice were euthanized at 5 or 7 days post-infection and organs were harvested for RNA isolation and histology. The left lung was fixed with 10% neutral buffered formalin for histology. The right lung lobes (superior, middle, inferior and post-caval) and nasal turbinates were homogenized in 1 mL of PBS and stored at -80°C until titration. To isolate mouse serum, blood was allowed to clot at room temperature for 30 min prior to clarifying by centrifugation at 15000 rpm in a tabletop centrifuge. Mouse serum was inactivated by 30 minutes incubation at 56°C to remove from the containment facility prior to further testing.

Detection of MCPT1 in mouse serum

Because mouse serum had been heat inactivated, potentially denaturing proteins, we used a western blot to detect MCPT1 levels in the blood. Serum was diluted 1:10 in PBS and denatured in 2x laemmli buffer (Bio-Rad, #1610737) before serum proteins were fractionated by SDS-PAGE. Proteins were then transferred on to PVDF membrane electrophoretically, which was blocked with 5% milk in TBST. Serum chymase was detected using Anti-Mast Cell Chymase antibody (Abcam, # ab2377, 1:250) and Goat anti-Mouse IgG (H+L) Cross-Adsorbed Secondary Antibody, HRP (ThermoFisher Scientific, #G21040, 1:10000). Densitometric analysis was done using Fiji (ImageJ, NIH).

Beta hexosaminidase assay

Purified His-Tag SARS-CoV-2 spike protein was obtained using a published protocol(6) and was used to coat polybead carboxylate microspheres (Polysciences Inc., Cat# 08226) as recommended by the manufacturer using 200 μ g of protein. The β -hexosaminidase assay was performed as previously described(7) with the following groups: bone marrow derived mast cells (BMMCs) obtained from C57Bl/6 mouse bone marrow + RPMI medium, BMMCs + ionomycin, BMMCs + spike-coated beads ratio 1:5, BMMCs + spike-coated beads ratio 1:15, BMMCs + spike-coated beads ratio 1:5 + Cromolyn (10 μ M), and BMMCs + spike-coated beads ratio 1:15 + Cromolyn (10 μ M). The absorbance at 405nm was measured with a plate reader (Spark 10M, Tecan). Percentage degranulation was calculated by dividing the absorbance in supernatant with the sum of absorbance in both supernatant and cell lysate.

Histology

Paraformaldehyde fixed tissues were snap frozen in O.C.T compound (Tissue-Tek, Sakura) and sectioned to 15 μ m thickness. For the toluidine blue staining protocol to identify MCs, sections were fixed in Carnoy's solution for 30 min at room temperature. Following fixation, sections were stained using 0.1% toluidine blue stain (Sigma-Aldrich, #198161) for 20 min and excess dye was removed by gently washing in running tap water followed by rinsing in distilled water. Sections were then dehydrated quickly in 95% alcohol followed by 2 changes in 100% alcohol and mounted using permanent mounting medium (VectaMount, #H-5000). For hematoxylin and eosin staining, air dried sections were rehydrated using a graded series of alcohol and stained using modified Harris hematoxylin (Sigma-Aldrich, #HHS32) for 10 min followed by a wash in tap water and two changes in distilled water. Sections were briefly dipped in 1% acid alcohol solution and quickly rinsed in distilled water before differentiating using 0.05% lithium carbonate solution for 1 minute. Sections were washed in distilled water and dehydrated using 95% alcohol followed by a counter stain using 0.25% eosin y (Sigma-Aldrich, #HT110232). Finally, sections were rinsed in 95% alcohol to remove excess eosin stain followed by 2 changes in 100% alcohol and air dried before mounted using permanent mounting medium (VectaMount, #H-5000). Images were obtained using a light microscope (Nikon) and processed using ImageJ Fiji.

Immunostaining of MCs

Tissue sections were permeabilized using 0.3% Triton X-100 in PBS for 30 min at room temperature followed by incubation with blocking buffer (0.1% Saponin+ 5% BSA in PBS) for 2h at room temperature. Mast cells were probed using heparin binding Avidin conjugated to FITC (BD Pharmingen, #554057) for overnight at 4°C. Sections were washed 3-4 times using PBS before mounting using Fluoroshield

mounting medium containing DAPI (Sigma-Aldrich, #F6057). Images were acquired using THUNDER Imaging Systems (Leica).

Clinical samples and microarray analysis

The data associated with human transcriptional responses was approved by the SingHealth Combined Institutional Review Board (CIRB 2017/2374). The detailed study design and protocol has been described previously(8), where whole blood transcript expression was measured in the severe and mild COVID-19 patients by the Affymetrix GeneChip Human Gene 2.0 ST Array. The raw data for the microarray profiling is available at Array Express (E-MTAB-9721), and the log2 counts are generated by the Transcriptome Analysis Console (Thermo Fisher), analyzed between the different days relative to peak severity with regards to respiratory function (Day 0). Temporal gene expression was analyzed by EDGE based on the log2 intensity counts(9), and genes that were significantly altered in the severe COVID-19 patients were identified based on p-value and q-value < 0.05. The genes from the MC-specific and the MC/Basophil phenotype were obtained from(10), and Partek® Genomics Suite® was used to tabulate the Least Square Means (LSMeans) values. Genes of increased expression during the acute phase or recovery phase were then further stratified. Normalized expression was tabulated by taking the average LSMeans values of all MC and MC/Basophil phenotype genes that were of increased expression during the acute phase. Heatmaps and graphs were constructed using Prism 9.0.2 software.

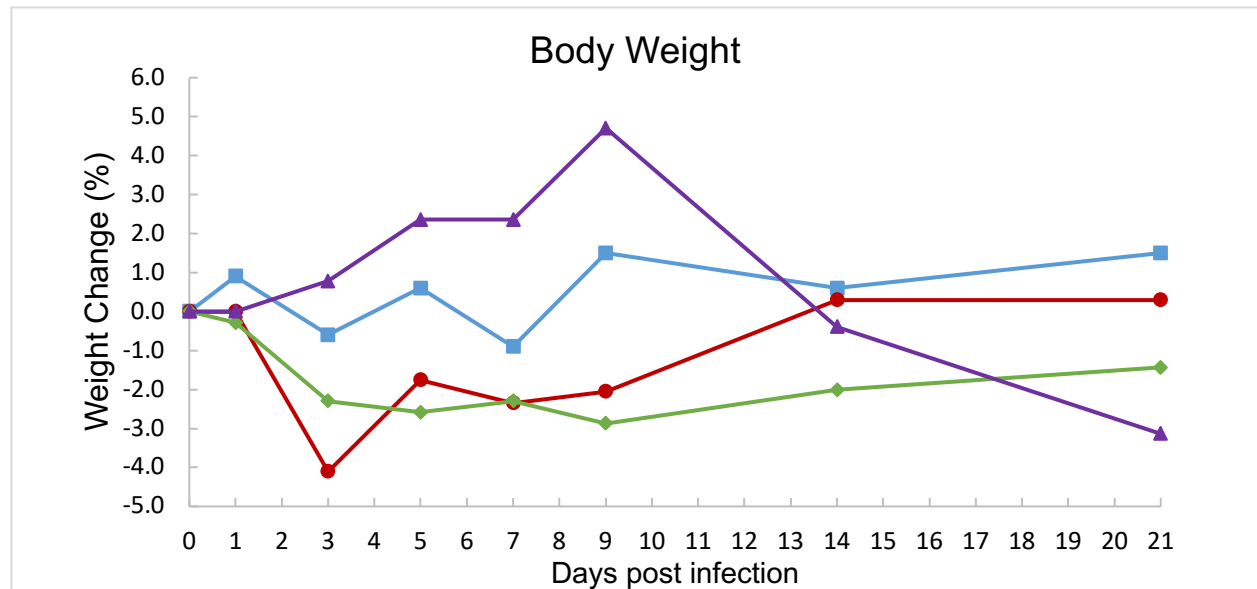
For analysis of the microarray or nCounter datasets, Z-score transformation was performed as described previously(11). To identify DEGs between symptomatic and asymptomatic subjects at baseline, Partek Genomics Suite Analysis v.7 software was used and Bonferroni's correction was performed based on the total number of 34,667 genes that were detected by microarray, using $P < 0.05$. No cutoff on fold change was imposed. For pathway analysis, the identified DEGs were used as input data, and analyzed against the Reactome database using the Enrichr tool(11). Both P values and combined scores for each enriched pathway were obtained from the Enrichr tool analysis using algorithms that are described in greater detail by Kuleshov et al.(11). Volcano plots were constructed using Prism v.8.1.0 software. To evaluate whether there was any statistically significant difference in specific Reactome pathways between symptomatic and asymptomatic subjects, the average Z-scores of all genes in each of the pathway were plotted. An unpaired, Student's t -test was then used to assess the statistical significance of the observed differences. The ROC curves for the various pathways were also determined using the average Z-scores of all genes in the UPR, sumoylation and TCA cycle pathway and plotted using Prism v.8.1.0. Ingenuity software was used to generate gene network diagrams.

Clinical samples for ELISA analyses

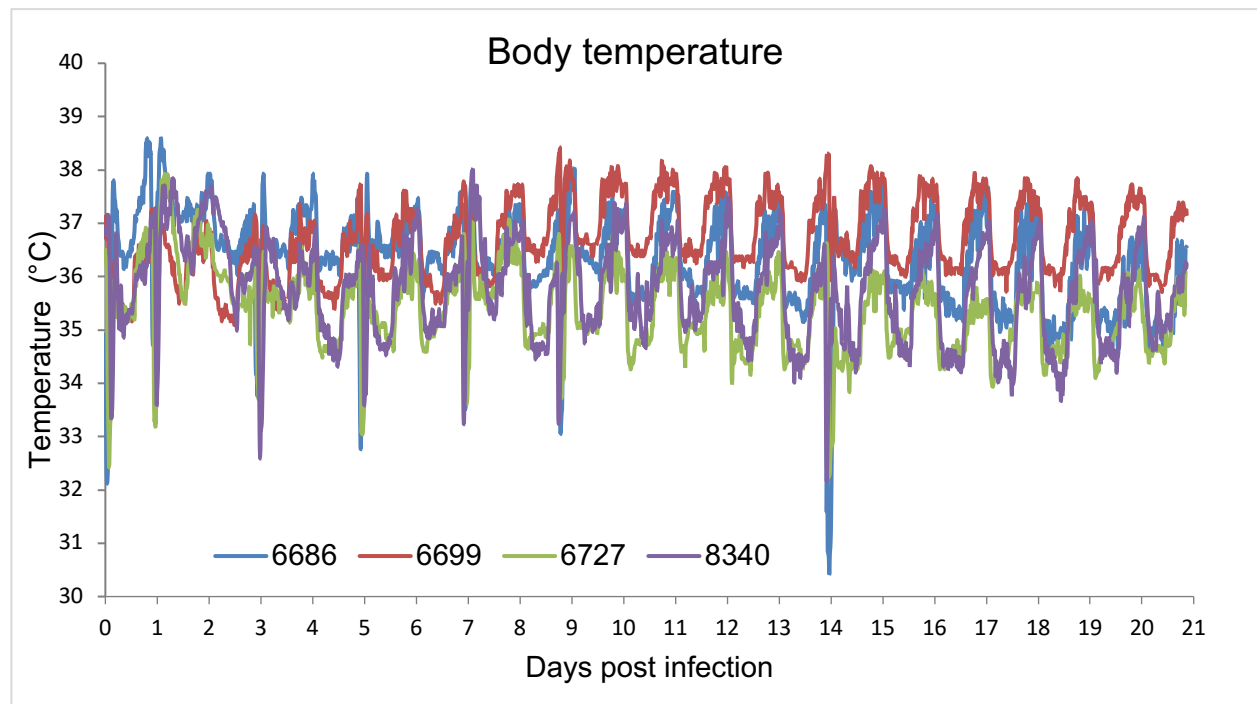
Patients with confirmed SARS-CoV-2 infection in either the hospital or outpatient setting were identified through the Duke University Health System (DUHS) or the Durham Veterans Affairs Health System (DVAHS) and enrolled into the Molecular and Epidemiological Study of Suspected Infection (MESSI, Pro00100241). Written informed consent was obtained from all subjects or legally authorized representatives. All plasma samples were from the time of enrollment with the exception of 1 patient whose sample was from day 3 and two subjects whose samples were from day 7 after enrollment. Peripheral blood was drawn into EDTA vacutainers, centrifuged, and isolated plasma was stored at -80°C until analysis. COVID-19 samples were processed under BSL2 with aerosol management enhancement and the following ELISAs were performed: chymase (Antibody Online, Aachen, Germany), Angiopoietin-1 and- 2 (ThermoFisher Science, Waltham, MA). A statistical analysis to confirm appropriate power was achieved was performed using SPSS and G*power software and outputs are provided in the "Supplemental Statistical Analysis" sub-section.

Patients with confirmed SARS-CoV-2 infection in Singapore were recruited in accordance with protocols approved by the intuitional IRB, DSRB domain E, (#2020/00120) and informed consent was taken from all patients. Approval was also obtained from the National University of Singapore IRB (NUS-IRB-2021-186). Serum samples from acute patients, <7 days of illness, were tested for chymase using the Human mast cell chymase I (CMA-I) kit (BlueGene Biotech, catalogue number E01M0368), according to manufacturer's instructions. Chymase concentration values obtained and previously published using the same kit for healthy control and DENV patients from Singapore(12) were compared to the values obtained in SARS-CoV-2 patients.

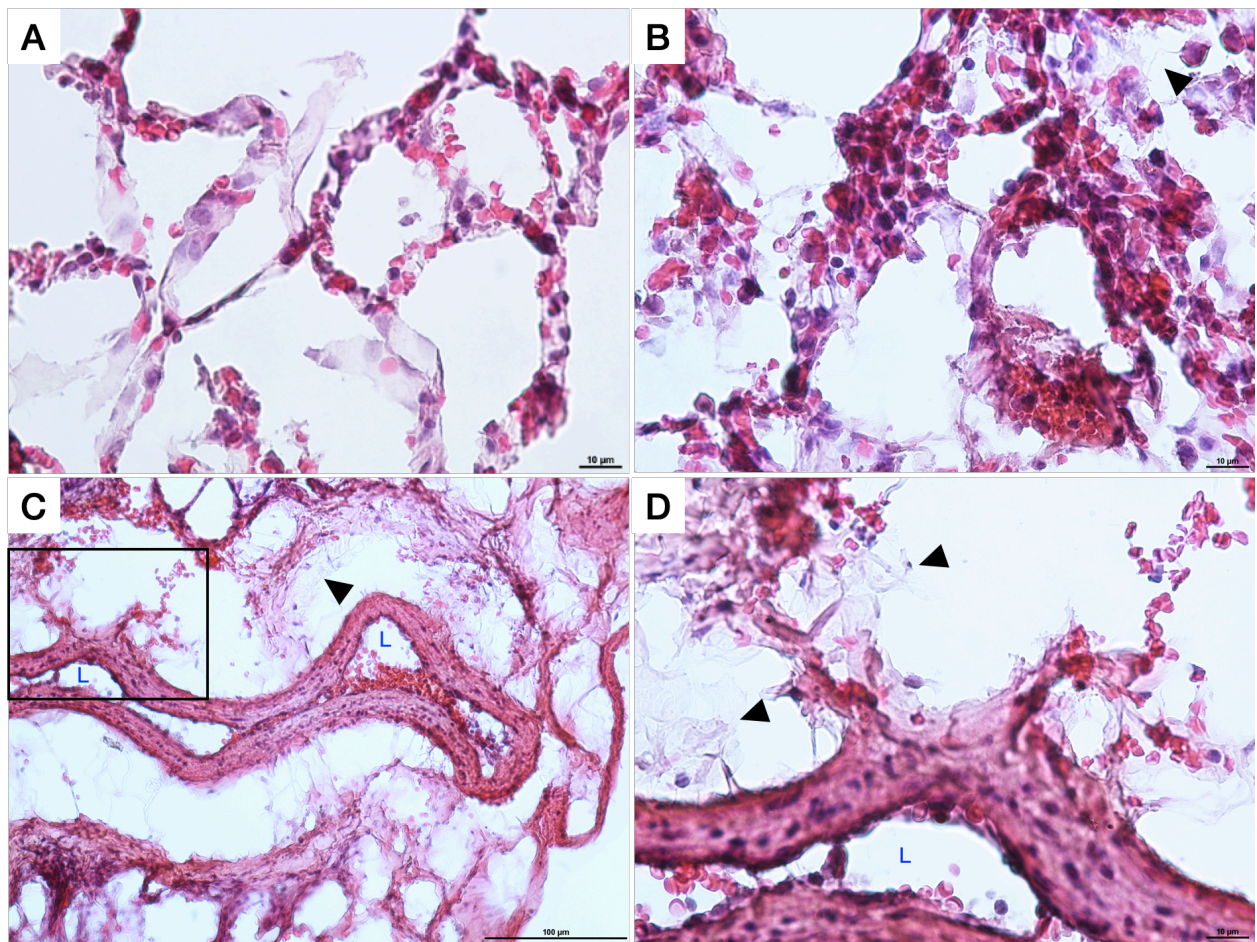
A



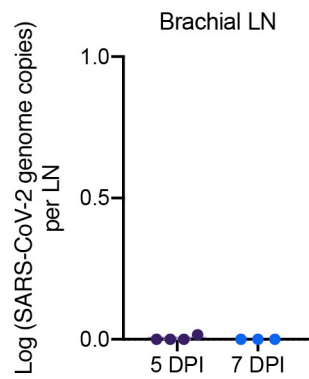
B



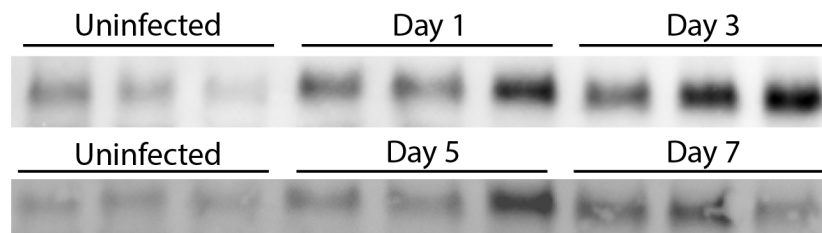
Supplemental Figure 1. Body weight and temperature in cynomolgus macaques infected with SARS-CoV-2. (A) Changes in body weight (% of initial weight) after infection with SARS-CoV-2. (B) Body temperature measured every 15 min by telemetry after infection. Dips in body temperature on D0, 1, 3, 5, 7, 9, and 14 are due to anesthesia administered for sample collection. Primate numbers are used to identify individual animals in the graph; $n = 4$.



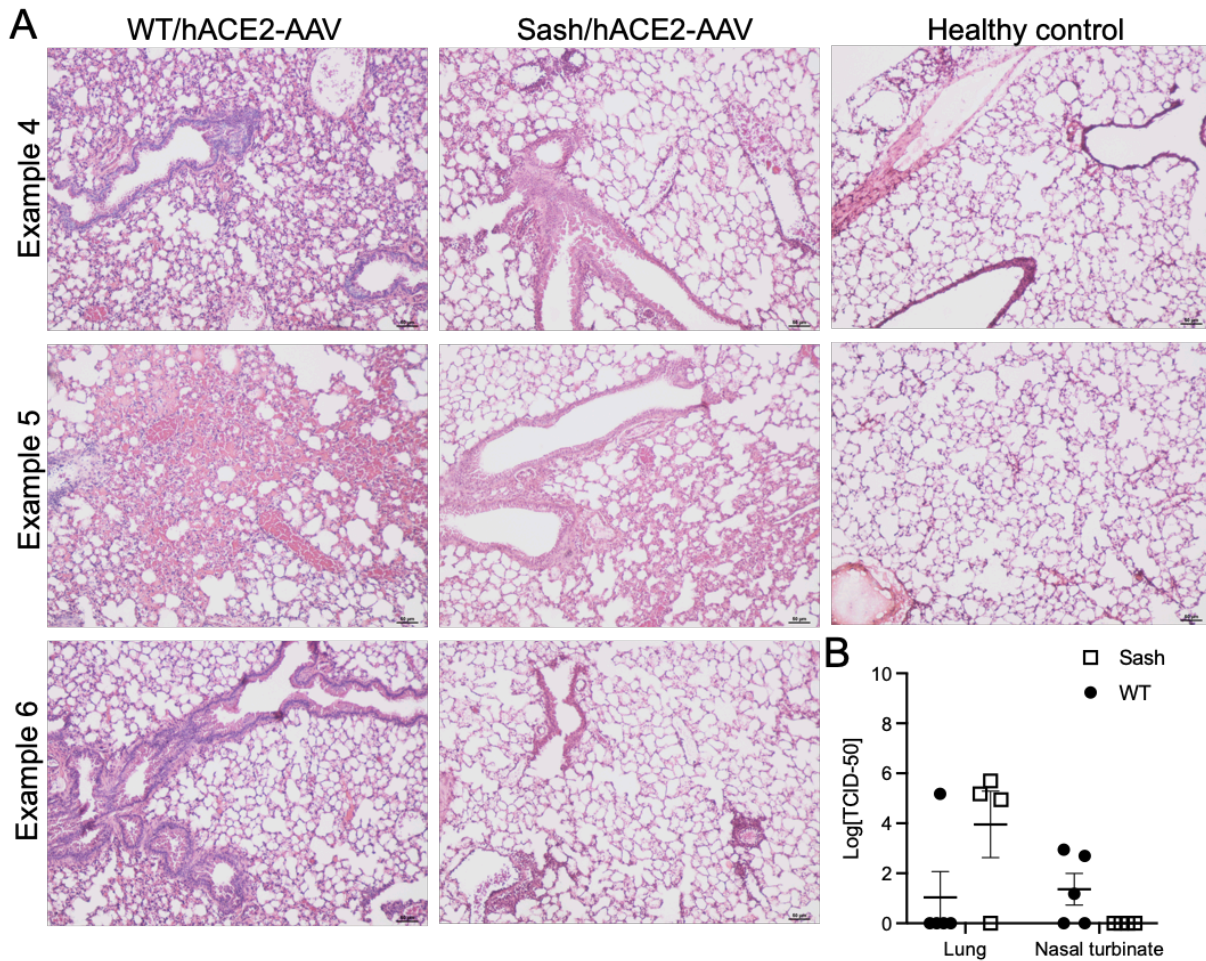
Supplemental Figure 2. Observation of hemorrhaging and coagulation in SARS-CoV-2-infected NHP lung alveoli. (A-B) Representative images showing the presence of free RBCs in the alveoli of NHPs 21d after SARS-CoV-2 infection. Notable thickening of the alveoli walls is observed in some sections, as in panel B. (C) Hemorrhaging from an artery in the lung is shown at low magnification (10x) and reimaged at higher magnification in panel D, corresponding to the boxed inset in C. For B-D, black arrows indicate examples of fibrin deposition in the tissue and for C-D, the artery lumen is indicated by a blue "L". Images are representative of observations from $n = 4$ primates.



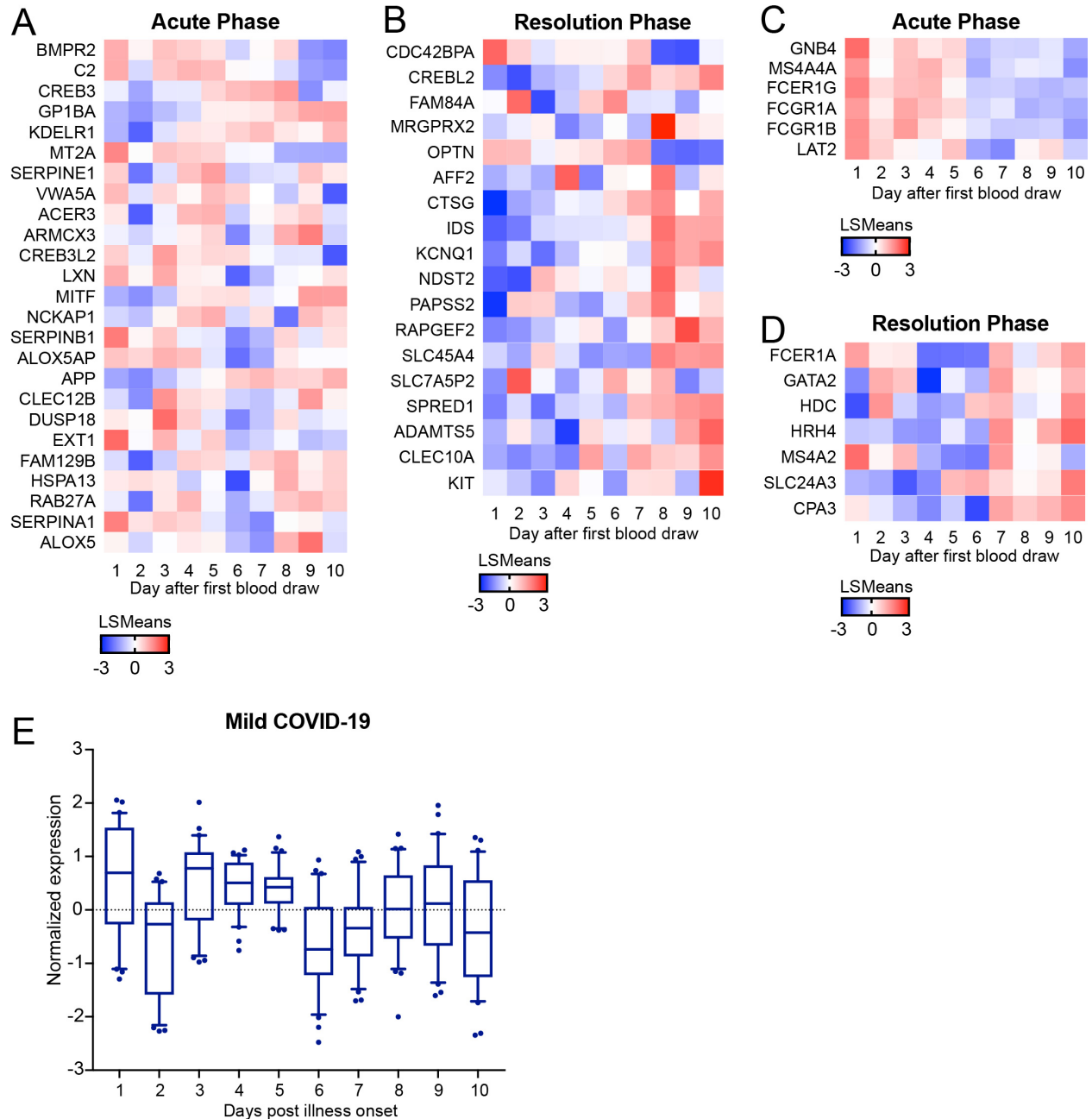
Supplemental Figure 3. No detection of SARS-CoV-2 in mouse brachial LNs days 5 or 7 post-infection.



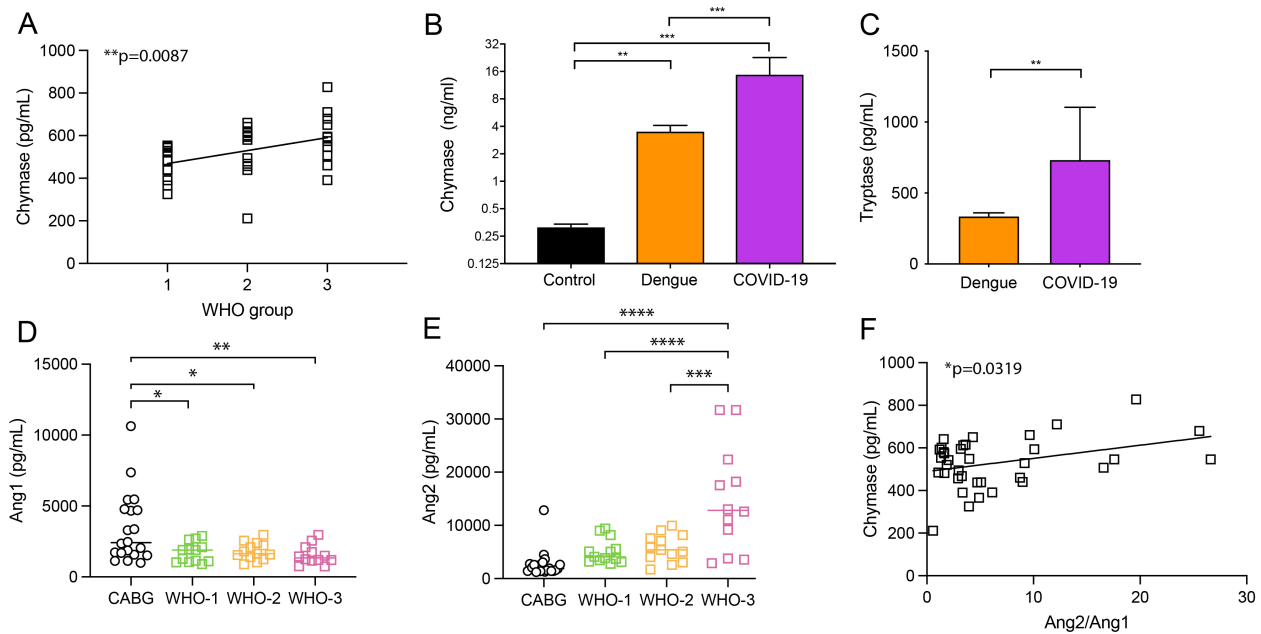
Supplemental Figure 4. MCPT1 detection in mouse serum. Additional replicates of western blots quantified in Figure 2E showing chymase detection in mouse serum Days 3, 5, and 7 post-infection. $n = 5$.



Supplemental Figure 5. Cellular infiltration observed in mouse lungs during SARS-CoV-2 infection. (A) Additional representative examples of lung tissue pathology during SARS-CoV-2 infection day 5 post-infection corresponding to **Figure 3, A and B**. Scale bars=50 μ M (B) Quantification of SARS-CoV-2 genome copies in lung homogenate and nasal turbinate by TCID50 showed no statistically significant differences in viral burden. Log-transformed data were compared by two-way ANOVA with Holm-Sidak's posttest and by multiple Mann-Whitney prior to log-transformation.



Supplemental Figure 6. Transcriptional responses of MC-associated genes in mild COVID-19 patients. Genes associated with a (A-B) MC-specific or (C-D) MC/basophil phenotype that were significantly regulated in severe COVID-19 patients are presented by heat map throughout the course of mild COVID-19 disease. Heatmap shows the LSmean expression values of mild COVID-19 patients ($n = 3$) over the course of illness. (E) Normalized expression levels of MC-specific expression in mild COVID-19 patients through the course of disease.



Supplemental Figure 7. Chymase and other biomarkers in COVID-19 patients. **A)** Correlation between disease severity according to WHO classification (**Figure 5B**) and plasma chymase concentration. Levels of **(B)** chymase and **(C)** tryptase in the serum of acute COVID-19 patients recruited in Singapore were compared to the concentrations previously detected and reported in a study of acute dengue patients(12) and healthy controls. Concentrations were compared by 1-way ANOVA with Bonferroni's post-test for panel B and Student's unpaired t-test for panel A to determine p-values. $n = 10$ for controls, $n = 108$ for dengue and $n = 3$ for COVID-19. For $**$, $p<0.01$; for $***$, $p<0.001$. **(D)** No change observed in Ang1 concentration between CABG controls and WHO severity group **(E)** while Ang2 concentrations were elevated in the WHO-3 group compared to all other groups and controls. **(F)** Correlation between plasma chymase concentration levels and Ang2/Ang1 ratios. For panels **(A, D-F)**, CABG patients $n = 20$; For WHO-1, $n = 13$; for WHO-2 $n = 13$; for WHO-3 $n = 12$.

DPI	% Neutralization			
	NHP 8340	NHP 6686	NHP 6699	NHP 6727
0	0.00	1.31	8.10	19.64
1	0.00	3.71	8.93	17.87
3	0.00	6.26	8.47	19.00
5	4.88	6.15	17.71	17.64
7	0.97	3.75	19.85	20.33*
9	5.23	38.75*	38.87*	47.64*
14	75.22*	89.75*	73.24*	86.37*
21	85.68*	91.37*	71.24*	88.76*

Supplemental Table 1. Surrogate virus neutralization test. Neutralizing activity was determined using an ELISA-based cPass™ kit that assessed antibodies blocking the interaction between RBD and ACE2 receptor. A cut-off of 20% inhibition (*) is used to identify seropositive samples.

	N	Sex (% Male)	Age	BMI	WHO 10 point score
Non-COVID-19	20	17 (75)	62.1±9.8	31.4±8.1	N/A
WHO group1	13	8 (61.5)	56.5±7.6	No Data	No Data
WHO group2	14	7 (50)	63.1±11.6	30.2±6.5	5 (IQR 1)
WHO group3	12	4 (33.3)	67.0±13.7	27,9±8.7	9 (IQR 0)

Supplemental Table 2. Demographics of COVID-19 patients and controls. Categorical variables are shown as absolute number (percentage), continuous variables as mean ± standard deviation, ordinal values as median (interquartile range: IQR). Community recruited patients constituting WHO group1, were asymptomatic or had mild symptoms at enrollment, but did not consent to medical record review, therefore available clinical data is limited.

Comorbidity	Non-COVID	WHO Group1	WHO Group2	WHO Group3
<i>Coronary Artery Disease</i>	20 (100)	N/A	3 (21.4)	1 (8.3)
<i>Congestive Heart Failure</i>	4 (20)	N/A	1 (7.1)	3 (25)
<i>Hypertension</i>	12 (60)	N/A	10 (71.4)	9 (75)
<i>Hyperlipidemia</i>	13 (65)	N/A	7 (50)	2 (16.7)
<i>Peripheral Vascular Disease</i>	4 (20)	N/A	2 (14.3)	2 (16.7)
<i>Diabetes Mellitus</i>	6 (30)	N/A	5 (41.7)	4 (33.3)
<i>COPD</i>	3 (15)	N/A	1 (7.1)	3 (25)

Supplemental Table 3. Patient co-morbidities. Categorical variables are shown as absolute number (percentage). Community recruited patients constituting WHO group1 did not consent to medical record review, therefore only limited clinical data is available.

Supplemental Statistical Analysis

Post-hoc power analysis using SPSS and G*Power

ANOVA						
CMA1	Sum of Squares	df	Mean Square	F	Sig.	Bayes Factor ^a
Between Groups	1365149.143	3	455049.714	34.248	<.001	5953580122.030
Within Groups	704209.283	53	13286.968			
Total	2069358.426	56				

a. Bayes factor: JZS method, testing model vs. null model.

Measures of Association

	Eta	Eta Squared
CMA1 * Group	.812	.660

G*Power results

Analysis:	Post hoc: Compute achieved power		
Input:	Effect size f	=	1.393
	α err prob	=	0.05
	Total sample size	=	58
	Number of groups	=	4
Output:	Noncentrality parameter λ	=	112.546
	Critical F	=	2.7757624
	Numerator df	=	3
	Denominator df	=	54
	Power (1- β err prob)	=	1.0000000

Supplemental References:

1. Ramakrishnan MA. Determination of 50% endpoint titer using a simple formula. *World J Virol.* 2016;5(2):85-6.
2. Chew WL, Tabebordbar M, Cheng JK, Mali P, Wu EY, Ng AH, et al. A multifunctional AAV-CRISPR-Cas9 and its host response. *Nat Methods.* 2016;13(10):868-74.
3. Aurnhammer C, Haase M, Muether N, Hausl M, Rauschhuber C, Huber I, et al. Universal real-time PCR for the detection and quantification of adeno-associated virus serotype 2-derived inverted terminal repeat sequences. *Hum Gene Ther Methods.* 2012;23(1):18-28.
4. Corman VM, Landt O, Kaiser M, Molenkamp R, Meijer A, Chu DK, et al. Detection of 2019 novel coronavirus (2019-nCoV) by real-time RT-PCR. *Euro Surveill.* 2020;25(3).
5. Lu X, Wang L, Sakthivel SK, Whitaker B, Murray J, Kamili S, et al. US CDC Real-Time Reverse Transcription PCR Panel for Detection of Severe Acute Respiratory Syndrome Coronavirus 2. *Emerg Infect Dis.* 2020;26(8).
6. Stadlbauer D, Amanat F, Chromikova V, Jiang K, Strohmeier S, Arunkumar GA, et al. SARS-CoV-2 Seroconversion in Humans: A Detailed Protocol for a Serological Assay, Antigen Production, and Test Setup. *Curr Protoc Microbiol.* 2020;57(1):e100.
7. St John AL, Rathore AP, Yap H, Ng ML, Metcalfe DD, Vasudevan SG, et al. Immune surveillance by mast cells during dengue infection promotes natural killer (NK) and NKT-cell recruitment and viral clearance. *Proc Natl Acad Sci U S A.* 2011;108(22):9190-5.
8. Ong EZ, Kalimuddin, S., Chia, W.C., Ooi, S.H., Koh, C.W.T., Tan, H.C., Zhang, S.L., Low, J.G., Ooi, E.E., Chan, K.R. Temporal dynamics of the host molecular responses underlying severe COVID-19 progression and disease resolution. *Ebiomedicine.* in press.
9. Storey JD, Xiao W, Leek JT, Tompkins RG, and Davis RW. Significance analysis of time course microarray experiments. *Proc Natl Acad Sci U S A.* 2005;102(36):12837-42.
10. Dwyer DF, Barrett NA, Austen KF, and Immunological Genome Project C. Expression profiling of constitutive mast cells reveals a unique identity within the immune system. *Nat Immunol.* 2016;17(7):878-87.
11. Kuleshov MV, Jones MR, Rouillard AD, Fernandez NF, Duan Q, Wang Z, et al. Enrichr: a comprehensive gene set enrichment analysis web server 2016 update. *Nucleic Acids Res.* 2016;44(W1):W90-7.
12. St John AL, Rathore, A. P. S., Raghavan, B., Ng, M. L., Abraham, S. N. Contributions of mast cells and vasoactive products, leukotrienes and chymase, to dengue virus-induced vascular leakage. *eLife.* 2013.